Proceedings World Geothermal Congress 2020+1
Reykjavik, Iceland, April - October 2021

Stochastic Modeling of EGS Using Continuum-Fracture Approach

Jan Březina, Pavel Exner, Jan Stebel and Martin Špetlík

Technical University of Liberec, Studentská 2, Liberec, 461 17, Czech Republic

jan.brezina@tul.cz, pavel.exner@tul.cz, jan.stebel@tul.cz, martin.spetlik@tul.cz

Keywords: EGS, DFN, stochastic modelling, hydraulic stimulation

ABSTRACT

Stochastic modeling of the hydraulic stimulation and long-term operation of an enhanced geothermal system (EGS) is performed. Both the stimulation model and the operation model consistently use the continuum-fracture approach. Stochastically generated fractures are used in a simple hydro-mechanical model of the stimulation process. The resulting system of fractures with significantly higher conductivity is used in the heat transfer model of the operation regime of the underground exchanger. This model is used to compute a single realization of the key EGS properties: the output power and temperature. Monte Carlo method is then applied to predict probabilistic distribution of the EGS properties. The conceptual model and input data are loosely based on the geologic properties at the Litoměřice site, possible location of the first EGS in the Czech Republic.

1. INTRODUCTION

As the natural hydrothermal resources are sparse in the Czech Republic, the EGS (enhanced geothermal system) concept is subject of the recent research focused on the usage of the geothermal energy. According to the available geological data (Čápová 2013), the Litoměřice site is the most attractive due to presence of a hot crystalline rock in relatively shallow depth. This motivates the implementation of the poroelastic model within the software Flow123d (Březina, Stebel and Exner, et al. 2011-2016), the simulator of the transport processes in fractured porous media. The study exploits this development to investigate uncertainty in the operational properties of EGS caused by the stochastic nature of the fracture system.

The EGS approach depends on opening and reconnecting of the preexisting fracture network in the low permeable rock induced by the hydraulic stimulation and the temperature changes. Since the fracture network is a-priori unknown as well as the spatial distribution of the essential parameters, we consider operational properties of the EGS as random variables. In order to predict their distribution, the Monte Carlo method can be applied, providing the forward model and the distribution of input parameters. Considering the forward model, three main approaches to the simulation of processes in a fractured porous media, namely single continuum, discrete fracture networks and continuum-fracture approach. The heterogeneous single continuum fully coupled THM model was used in (Watanabe, et al. 2009) to study uncertainty in the output temperature caused by spatially random input fields. The DFN approach essentially uses random fractures and thus is often combined with the Monte Carlo method, see e.g. (Ezzedine 2010). We adopt the continuum-fracture approach that is much less common especially for significantly more demanding implementation. In (Doonechaly, Azim and Rahman 2016) this approach was used for sensitivity analysis of the EGS operation, but only within a fixed fracture network.

We consider a simple two stage forward model. At first the hydraulic stimulation is described by the hydro-mechanical (HM) poroelastic model combining the discrete fractures and the continuum. Linear elasticity is used, contact conditions and thermal effects are not considered, although these may have significant impact. Based on the stimulation model, the changed aperture and conductivity fields on the fractures are determined. Then the evolution of the temperature and the raw power output is simulated using the combined fracture-continuum approach for the thermo-hydraulic (TH) model as well. A realistic stochastic model for the distribution of the fractures is considered, while the other parameters are fixed as we want to study the influence of variability in the fracture network in particular.

2. CONCEPTUAL MODEL

According to available geological data for the Litoměřice site, see (Čápová 2013), the crystalline bedrock possibly consisting of granite, gneiss or mica schist is located in the depth below 3 km. Two geological scenarios lead to predicted temperatures in the depth of 5 km: 140 °C and 146 °C, respectively. In this depth, we consider two vertical wells in distance 200 m with opened part of the length 100 m. The simulation domain is a box with dimensions $600 \times 600 \times 600$ m covering only the close neighborhood of the fractured volume with the two wells placed in its center. In order to reduce the complexity of the computational mesh, we cut off cylinders of the radius 10 m at the wells positions and apply boundary conditions on their walls while avoiding very fine meshing at the wells scale. This approximation is discussed in detail in Section 0. This simplified geometry is consistent with the simplification in the mathematical model as the precision of the model prediction is not of our interest in this work. We refer to the contribution paper (Rálek, et al. n.d.) for the more thorough EGS study of the Litoměřice site.

3. HYDRO-MECHANICAL MODEL

During the hydraulic stimulation the fluid is injected into both wells in order to open the preexisting fractures. This leads to increase of aperture of the fractures, which is then used in the production phase model described in the next section. As the HM model of 3d rock we use the Biot poroelasticity equations:

$$\partial_t \left(Sp + \alpha \operatorname{div} \boldsymbol{u} \right) + \operatorname{div} \boldsymbol{q} = 0, \qquad - \operatorname{div} \boldsymbol{\sigma} + \tilde{\iota} \tag{1.1}$$

Here $\boldsymbol{u}$ is the displacement [m], p is the pressure head [m], $h = p + x_3$ is the piezo-metric head and the flux $\boldsymbol{q}$ [m.s $^{-1}$] is given by the Darcy law

$$\boldsymbol{q} = -k \nabla h \tag{1.2}$$

with the hydraulic conductivity k . The coefficient $\tilde{\iota}$ ñ where α is the Biot's effective stress parameter (Biot 1941), ρ_l is liquid density and g is gravitational acceleration. The stress tensor $\boldsymbol{\sigma}$ [Pa] is given by the Hook's law for the isotropic material:

$$\boldsymbol{\sigma} = \mathbf{C} : \grave{\mathrm{o}} = (\lambda_M \mathbf{I} \otimes \mathbf{I} + 2\mu_M \mathbf{I}) : \grave{\mathrm{o}}; \qquad \grave{\mathrm{o}} = (\nabla \boldsymbol{u}^T + \nabla \boldsymbol{u}) / 2 \tag{1.3}$$

where $\mu_M = E / \left(2(1+\nu)\right)$ and $\lambda_M = E\nu / \left((1+\nu)(1-2\nu)\right)$ are the Lammé parameters [Pa].

The continuum-fracture approach consists in integration of the governing equations across the volume of a thin fracture effectively reducing its dimension to a 2d surface. This procedure was introduced by (Martin, Jaffré and Roberts 2005) for the Darcy flow and extended for general advection-diffusion process in (Březina and Stebel, Analysis of Model Error for a Continuum-Fracture Model of Porous Media Flow 2015). For the purpose of this work, the same approach was applied also to the equations of linear elasticity. We introduce the unit normal vector $\boldsymbol{v}$ to the fracture plane with arbitrary but fixed orientation. For a general quantity s that is defined on both faces of the fracture volume, we define the jump □ □ s^-, where $s^\pm$ are the traces of s on the faces. Then integrating (1.1) across the fracture aperture results in the following system of equations:

For the 2d fractures we apply a dimension reduction procedure, which was originally developed in (Martin, Jaffré and Roberts 2005) for the Darcy flow. We introduce the unit normal vector $\boldsymbol{v}$ to the fracture plane with arbitrary but fixed orientation. For a quantity, say p, which is defined on both sides of the fracture, we define the jump □ □ p^-, where $p^\pm$ is the trace of p on the positive/negative side of the fracture, determined by the orientation of $\boldsymbol{v}$. Then, integrating (1.1) across fracture aperture results in the following system of equations:

$$\begin{aligned} \delta\Big(\partial_t\Big(S_f p_f + \alpha_f\Big(\mathrm{div}_\tau \boldsymbol{u}_f + \tfrac{1}{\delta}\square\ \square \quad {}_f \Delta_\tau h_f\Big) = \square\ \square \\ \delta\Big(-\mathrm{div}_\tau \mathbf{C}_f\Big(\nabla_\tau \boldsymbol{u}_f + \tfrac{1}{\delta}\boldsymbol{v} \otimes \square \quad {}_f \Big) : \square\ \square \end{aligned} \tag{1.4}$$

Here p_f and $\boldsymbol{u}_f$ is the average pressure head and the average displacement on the fractures, respectively. The subscript τ indicates tangential operators on the fracture plane, $\otimes$ denotes the outer product and $\tilde{\iota}$ ñ g. The jumps □ □ F^- and □ □ $\boldsymbol{Q}^-$ are water sources and the forces that arise from the approximation of derivatives in the normal direction:

$$\begin{aligned} F^\pm &:= \pm\frac{2}{\delta} k_f \left(h^\pm - h_f\right), \\ \boldsymbol{Q}^\pm &:= \pm\frac{2}{\delta} \mathbf{C}_f \Big(\nabla_\tau \boldsymbol{u}^\pm + \boldsymbol{v} \otimes \left(\boldsymbol{u}^\pm - \boldsymbol{u}_f\right)\Big)\boldsymbol{v}. \end{aligned} \tag{1.5}$$

System (1.1) and (1.4) is complemented by the boundary conditions for the bulk domain prescribed on the fracture faces:

$$k \nabla h^\pm \cdot \boldsymbol{v} = F^\pm, \qquad \left(\mathbf{C}\left(\nabla \boldsymbol{u}^\pm\right) - \tilde{\iota} \quad \right) \boldsymbol{Q}^\pm. \tag{1.6}$$

For the sake of simplicity we stimulate both wells simultaneously which results in very similar change of the fracture aperture as if the wells were stimulated one by one. Zero piezometric head and zero displacement are used as the initial conditions. The liquid is injected for 1 day under the stimulation pressure of 50 MPa (piezometric head $h_s = 5 \times 10^3$ m). This pressure is not applied directly on the surface of the well's cylinders, but through the Robin boundary condition with the transition parameter derived from the approximate analytical solution at the vicinity of the well. The zero piezometric head is prescribed on the box sides, while the no flow condition is applied on the top and bottom face. Following boundary conditions were applied for the elasticity equation: zero displacement on the bottom of the box, zero normal displacement on the well's cylinders and zero traction elsewhere.

4. THERMO-HYDRAULIC MODEL

The TH model describes the heat transport in the EGS through the operation phase within 30 years after the hydraulic stimulation performed according to Section 0. In this scenario, we consider a steady Darcy flow:

$$\mathrm{div}\ \boldsymbol{q} = 0, \qquad \mathrm{div}\boldsymbol{q}_f = \square\ \square \quad = -\tilde{\iota} \ldots, \tag{1.7}$$

for the bulk domain and fractures, respectively. The fracture aperture $\tilde{\iota}$ is updated according to the HM model. The conductivity of the fractures is also adjusted according to the cubic law $\ldots \tilde{\iota} \ldots$. The communication between the fractures and the bulk rock is defined by the conditions (1.5) and (1.6).

The heat transport model is sequentially coupled with the hydraulic model using computed Darcy flux $\boldsymbol{q}$ and $\boldsymbol{q}_f$. It assumes thermodynamic equilibrium between the liquid and the rock, the advection-diffusion equation for the bulk and fracture domain reads:

$$\begin{aligned} \partial_t\left(\tilde{\ } \quad \tilde{\mathrm{n}}_l c_l T \boldsymbol{q}\right) - \operatorname{div}\left(\lambda \nabla T\right) = 0, \\ \partial_t\left(\delta \tilde{\ } \quad \mathrm{v}\left(\tilde{\mathrm{n}}_l c_l T_f \boldsymbol{q}_f\right) - \operatorname{div}\left(\delta \lambda_f \nabla T_f\right) = \square \ \square \end{aligned} \tag{1.8}$$

Here T [°C] is the temperature, $\tilde{\mathrm{n}}_l$, $\tilde{\mathrm{n}}_s$ is the density, c_l, c_s is the heat capacity and

$$\tilde{\ } \quad \tilde{\mathrm{n}}_{\cdot} \cdot \left(1-\vartheta\right)\tilde{\mathrm{n}}_s c_s, \quad \lambda = \vartheta\lambda_l + \left(1-\vartheta\right)\lambda_s, \tag{1.9}$$

where θ is the porosity and λ_l, λ_s is the thermal conductivity.

Similarly to (1.5), we obtain the relationship for the normal heat fluxes on the fracture faces:

$$G^{\pm} := \pm\frac{2}{\delta}\lambda_f\left(T^{\pm} - T_f\right) + \tilde{\mathrm{n}}_l c_l F^{\pm} T_q, \tag{1.10}$$

where T_q is equal to the temperature in the bulk or fractures as the normal Darcy flux $F^{\pm}$ is positive or negative, respectively. The system is completed by the bulk boundary conditions:

$$-\left(\rho_l c_l \boldsymbol{q} T_q - \lambda \nabla T^{\pm}\right) \cdot \boldsymbol{\nu} = G^{\pm}. \tag{1.11}$$

The liquid is continuously injected into the left well under the pressure 0.5 MPa ($h_i = 50$ m) and pumped out to the level of the EGS ($h_o = -5000$ m). No flux condition is used on the outer boundary. The injecting temperature is set to 15 °C, the natural convection heat flux is prescribed on the production well. The initial temperature field is considered on the outer boundary, which is given by 10 °C at the Earth surface and the geothermal gradient 30 °C.km^{-1}.

5. GEOLOGY AND MODEL PARAMETERS

Most of the parameters used for computation are gathered in Table 1 Physical parameters of rock, fractures and water, used in the model.. The mechanical properties of granitic rocks have been investigated e.g. in (Ljunggren, et al. 1985), where the measured Young modulus E varies around 50 GPa and the Poisson's ratio ν is around 0.25. The Biot's coefficient for different rocks is hard to obtain, we use the value $\alpha = 0.6$ inspired by (Selvadurai, Selvadurai and Nejati 2019), where α for Grimsel granite varies between 0.46 to 0.72. The reported values of the drained compressibility β of several types of granite and orthogneiss are approx. 20×10^{-13} cm^2.dyne^{-1} = 2×10^{-11} Pa^{-1} (Zisman 1933). As far as porosity ϑ is concerned, (INTERA Environmental Consultants and Houston 1983) reports values between 0.001 and 0.01 for metamorphic crystalline rocks, we shall consider the value 0.005. We assume the standard value of the gravitational acceleration $g = 9.81$ m.s^{-2}. The storativity S is calculated from the water compressibility $\beta_l = 5\times10^{-10}$ Pa^{-1} and the porosity following (Brace, Walsh and Frangos 1968), (INTERA Environmental Consultants and Houston 1983):

$$S = \tilde{\mathrm{n}}_l g(\beta + \vartheta\beta_l) \approx 2\times10^{-7} \text{ m}^{-1}. \tag{1.12}$$

The values of physical parameters in the fractured zone are mostly unknown, hence the following values are only approximate. The aperture of the fractures is considered constant in the input of the HM model. The elastic modulus of fracture is assumed much smaller than in the bulk rock, $E_f = 50$ Pa. After the process of the hydraulic fractioning, the aperture and hydraulic conductivity are adjusted according to the displacement results, see TH model in (1.7). The porosity is taken much higher than in the rock due to the increased k_f, i.e. we consider $\vartheta_f = 0.8$. We assume the same compressibility $\beta_f = \beta$, which gives approximately the same value of storativity $S_f \approx S$.

The hydraulic conductivity k in the bulk rock is set similarly to (Šperl and Trčková 2008) and (Doonechaly, Azim and Rahman 2016), where they also consider DFN and surrounding rock. Additionally we assume that the hydraulic fractioning impacts also the smaller fractures not included in our DFN, so we increase $\tilde{\ }$ m.s^{-1} of the bulk rock.

	Rock	Fractures	Liquid
Young modulus E [Pa]	50×10^9	50	--
Poisson's ratio ν [--]	0.25	0.25	--
Biot's coefficient α [--]	0.6	0.6	--
Density ñ [kg.m^{-3}]	2700	2700	1000
Porosity ϑ [--]	0.005	0.8	--
Compressibility β [Pa^{-1}]	2×10^{-11}	2×10^{-11}	5×10^{-10}
Storativity S [m^{-1}]	2×10^{-7}	2×10^{-7}	--
Cross-section δ [m]	--	$*\,5\times10^{-5}$	--
Hydraulic conductivity k [m.s^{-1}]	$*10^{-9}$	$*\,2.5\times10^{-3}$	--
Heat capacity c [J.kg^{-1}.K^{-1}]	790	790	4000
Thermal conductivity λ [W.m^{-1}.K^{-1}]	2.5	2.5	0.5

Table 1 Physical parameters of rock, fractures and water, used in the model.

6. ANALYTICAL MODELS IN THE VICINITY OF THE WELL

In order to keep the mesh size treatable, we cut out of the computational domain two cylinders around the open well parts with a larger radius $R = 10$ m. On the surface of these cylinders we consider the Robin type boundary condition for the piezometric head:

$$k\nabla h \cdot \boldsymbol{n} = \sigma(H_w - h), \tag{1.13}$$

where $\boldsymbol{n}$ is the unit normal vector pointing to the center of the well and H_w is the piezometric head in the well. The parameter σ is determined from the analytical radially symmetric solution of the steady Darcy flow problem with a point source:

$$\hat{h}(r) = -\alpha \log(r) + \beta, \tag{1.14}$$

where r is the distance from the well and α, β are arbitrary constants such that $\hat{h}(\rho) = H_w$ holds. First, the flux from the well into the domain through the surface C_ρ of the cylinder with radius ρ and length L is

$$Q_\rho := -\int_{C_\rho} k\nabla h \cdot \boldsymbol{n} = -2\pi\rho L k\hat{h}'(\rho) = 2\pi L k\alpha. \tag{1.15}$$

Next, the flux at the distance *R* can be expressed from (1.13) as follows:

$$Q_R = 2\pi RL\sigma(\hat{h}(\rho) - \hat{h}(R)) = 2\pi RL\sigma\alpha \log(R/\rho). \tag{1.16}$$

Finally, since $Q_\rho = Q_R$, we obtain from (1.15) and (1.16):

$$\sigma = \frac{k}{R\log(R/\rho)}. \tag{1.17}$$

In the simulations we shall use the hydraulic conductivity of the fractures in (1.17) as the fractures have major influence on the flow in the vicinity of wells.

Since the heat transfer is dominated by the convection in the vicinity of the wells, the temperature in the well is transported to the surface of the cut-off cylinders or vice versa in the time $t_0 = R/q$ which for the observed volume fluxes $Q \sim 1$ l/s is about 100 days. This is negligible with respect to the total lifetime of the heat exchanger, hence in the simulation of heat we shall use Dirichlet boundary condition for the temperature.

7. STOCHASTIC DESCRIPTION OF THE FRACTURES

The fracture stochastic model consists of the Fisher's distribution for the fracture orientation, the power law for the fracture size, Poisson process for the number of fractures and uniform distribution for the fracture centers. The square fractures are considered with the side $r/2$. The von Mises-Fischer distribution (Fisher/Lewis/Embleton, Statistical Analysis Spherical Data 1993) is used to describe orientation of single family of fractures with given mean normal vector $\boldsymbol{a}$ and the concentration parameter κ. The distribution is radially symmetric around $\boldsymbol{a}$ with the density function for the angle θ between $\boldsymbol{a}$ and fracture normal:

$$f(\theta) = c_\theta \exp\big(\kappa\cos(\theta)\big)\sin(\theta), \quad c_\theta = \frac{\kappa}{2\pi\big(\exp(\kappa)-\exp(-\kappa)\big)}. \tag{1.18}$$

The power law distribution is considered for the fracture size r. This kind of distribution is scale invariant, which is the key property of the natural fracture networks, see (Bonnet, et al. 2001) for detailed discussion. In practice the scale invariance holds only on some range of scales, leading to the truncated power law with the density:

$$f(r) = c_r r^{-(\gamma+1)}, \quad \frac{1}{c_r} = \int_{r_0}^{r_1} r^{-(\gamma+1)} dr = \frac{r_0^{-\gamma} - r_1^{-\gamma}}{\gamma}, \tag{1.19}$$

for $r \in [r_0, r_1]$. For the given scale range, the number of fractures in unit volume is described by the Poison process with the intensity $\lambda = P_{30}[r_0, r_2]$ describing the mean number of fractures in the unit volume. The measurable parameter is the related mean total area per unit volume

$$P_{32} = \int_{r_0}^{r_1} r^2 f(r) dr = P_{30} \frac{\gamma}{2-\gamma} \frac{r_0^{2-\gamma} - r_1^{2-\gamma}}{r_0^{-\gamma} - r_1^{-\gamma}}. \tag{1.20}$$

In order to obtain fracture sets of the size tractable by our simulation tools, we represent explicitly only the fractures in the scale range $[r_2, r_3]$ while the scales $[r_0, r_1]$ are treated as equivalent porous media. The upper bound r_3 is set to the diameter of the simulation domain and upper scales are omitted. The lower bound is determined by desired mean intensity $P_{30}[r_2, r_3]$ through the relation:

$$\frac{P_{30}[r_2, r_3]}{P_{30}[r_0, r_1]} = \frac{r_2^{-\gamma} - r_3^{-\gamma}}{r_0^{-\gamma} - r_1^{-\gamma}}. \tag{1.21}$$

Positions of the fracture centers are sampled uniformly over the smaller box around the wells with dimensions $(300,150,150)$.

Since no fracture statistics data for the target locality are available, we use data for the Forsmark site in Sweden (Follin 2008) with a crystalline bedrock. Parameters of the distributions for five families of the fractures are summarized in Table 2 Used stochastic parameters of the five fracture families. Parameters of the distributions of the fracture orientation, size and intensity..

SKB data - FFM01 and FFM06 (depth 0 to -200 m)								
FFM01a		Fisher orientation			Power law			
Set	Name	Trend [°]	Plunge [°]	Conc. [-]	r_0 [m]	k_r [-]	r_{max} [m]	$P_{32}[r_0, r_{max}]$ [$m^2.m^{-3}$]
1	NS	292	1	17.8	0.038	2.50	564	0.073
2	NE	326	2	14.3	0.038	2.70	564	0.319
3	NW	60	6	12.9	0.038	3.10	564	0.107
4	EW	15	2	14.0	0.038	3.10	564	0.088
5	HZ	5	86	15.2	0.038	2.38	564	0.543

Table 2 Used stochastic parameters of the five fracture families. Parameters of the distributions of the fracture orientation, size and intensity.

8. NUMERICAL RESULTS

The model described above is used to sample the production temperature and the heat power in the period of 30 years with 1 year time step. A single execution of the forward model consists of the following steps:

- draw a fracture set sample according to Section 5.2
- create the geometry with fracture intersections and generate a mesh using own Python code and GMSH meshing tool (Geuzaine and Remacle 2009)
- perform custom mesh healing algorithm to improve mesh quality

- execute the HM model in Flow123d
- compute the modified aperture and hydraulic conductivity in the fractures
- execute the TH model in Flow123d with opened fractures
- execute the TH model in Flow123d with unmodified fractures (reference sample)

An example of a single realization of the fracture network can be seen in Figure 1. The confinement of the fracture centers to a box around the wells is clearly visible, we obtain pretty good intersection with the well cylinders but the fracture network typically does not create a connect path between the wells. Due to technical reasons, we use the expected number of fractures 100 and set r_2 accordingly using (1.21), approximately 30 m. The domain diameter is used for the upper fracture size limit $r_3 = 600$ m. We do not expect significantly better connectivity of the fracture network for larger number of fractures due to the nature of the power law which permits adding only smaller fractures. The temperature distribution on the fractures and on the vertical cut of the domain after 5 years can be seen in Figure 1 and Figure 2. The influence of the fractures on the heat transfer in the bulk domain is clearly visible.

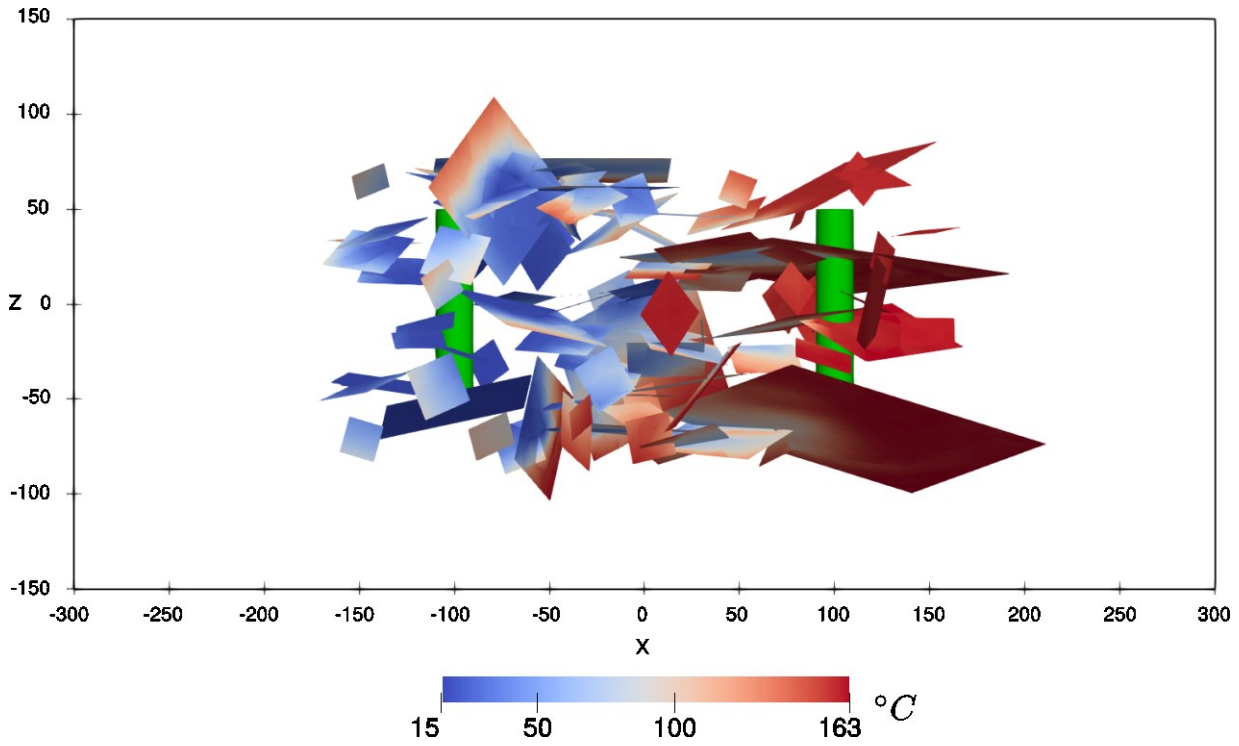

Figure 1: A fracture set sample with distribution of the temperature after 5 years of the operation with the stimulated fractures. The open parts of the wells are denoted in the green color.

Total number of 1000 executions of the complete forward model was performed using a parallel cluster. These models used a precomputed set of good quality meshes that were selected from about 2000 independent fracture sets. Further, around 100 samples were rejected because of the unrealistic temperatures caused by the instability of the used numerical method for some extremely heterogeneous cases of the modified conductivity of the fractures. Remaining samples were used to estimate the mean and the standard deviance for the output temperature and the output power. Evolution of the mean and standard deviance is plotted in Figure 3.

The histograms for the selected times 1, 15 and 30 years are in Figure 4. Absolute values especially for the power may not be realistic, but the important observation is the relation between the standard deviation and the gap between the stimulated and the reference case. As can be seen from the histograms, the distribution for power is close to normal just slightly skewed for the initial times. Thus the standard variance corresponds to about 70 % of samples, say otherwise: doing the stimulation there is a 15 % chance you get the power below the plotted standard deviation band, which is not very small probability and the value is already pretty close to the reference non-stimulated case.

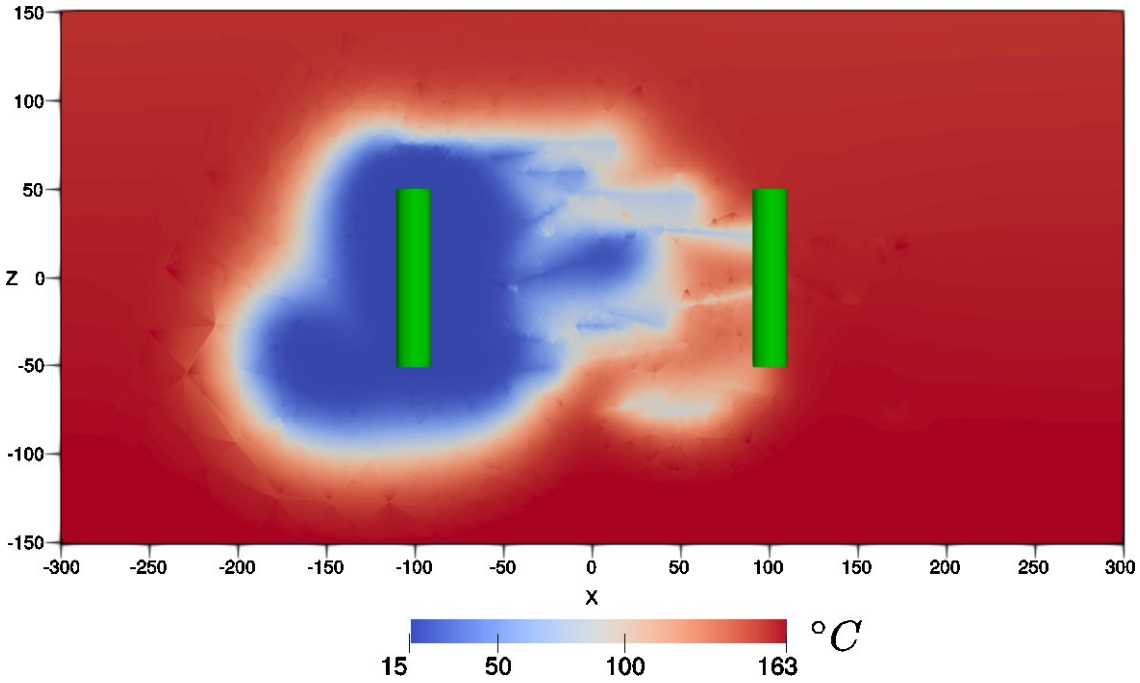

Figure 2: A single sample of distribution of the temperature in the bulk domain after 5 years of operation with the stimulated fractures. The open parts of the wells are denoted in the green color.

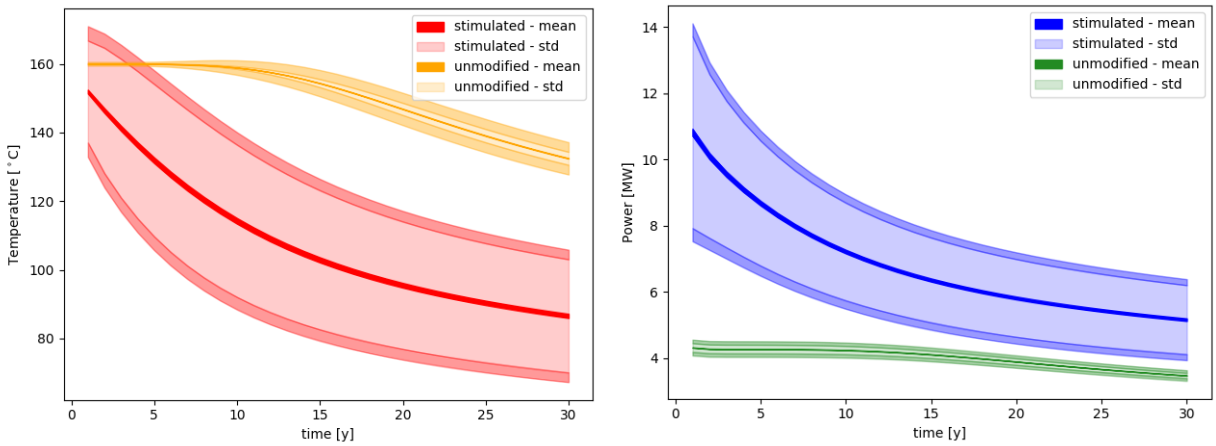

Figure 3: Evolution of the estimated mean output temperature and the output power for the stimulated and unmodified fracture network. The band width is the error of estimation the wide transparent band is the estimate of the standard variance due to the fracture dispersion again with outer band marking the error of the estimation.

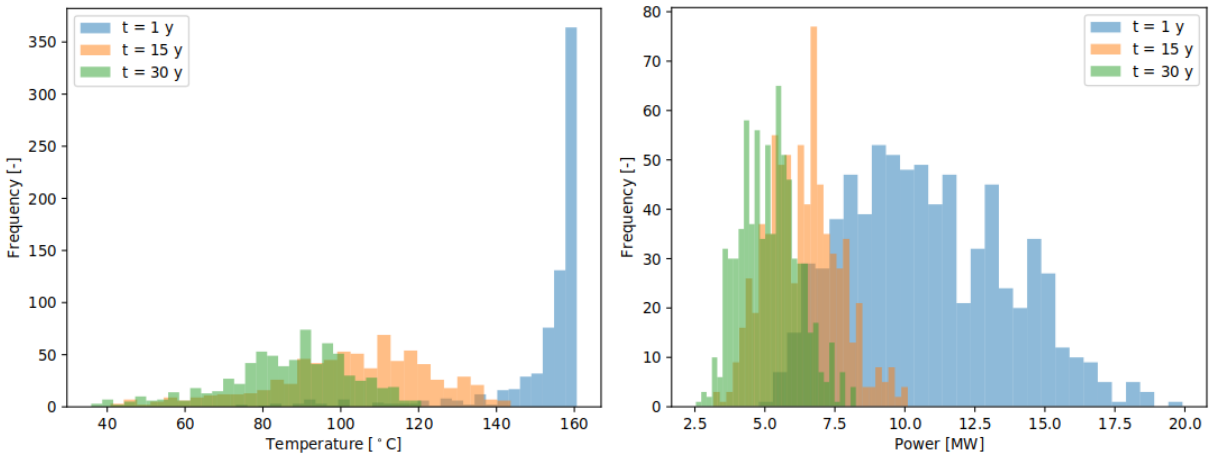

Figure 4: Histogram of the output temperature and power in 1,15, and 30 years of operation with the stimulated fractures

9. CONCLUSIONS

We have developed the HM model for the hydraulic stimulation and the TH model for the heat transfer using consistently the continuum-fracture approach. Although the model is conceptually simple, it neglects important thermal effects and contact conditions during the stimulation, it is yet capable to reproduce a significant effect of the fracture stimulation on the output power and temperature compared to the reference case without stimulation.

We have shown, that the uncertainty of the power due to fracture dispersion is relatively high in the comparison to the power increase caused by the stimulation. It may indicate relatively high probability that the stimulation may not result in sufficiently high power for the long term production phase. Further research may investigate if the multiple stimulations can deal with such cases.

ACKNOWLEDGEMENT

a) RINGEN: The research was supported by the Czech Ministry of Education, Youth and Sports under the project No. LM2015084.

b) RINGEN+: The research was supported by the project No. CZ.02.1.01/0.0/0.0/16_013/0001792, co-funded by the EU Operational Program “Research, Development and Education”.

REFERENCES

Baghbanan, Alireza, a Lanru Jing. „Hydraulic Properties of Fractured Rock Masses with Correlated Fracture Length and Aperture.“ *International Journal of Rock Mechanics and Mining Sciences* 44 (7 2007): 704-719.

Biot, Maurice A. "General Theory of Three-Dimensional Consolidation." *Journal of Applied Physics* 12 (2 1941): 155-164.

Bonnet, E., et al. "Scaling of Fracture Systems in Geological Media." *Reviews of Geophysics* 39 (2001): 347-383.

Brace, W. F., J. B. Walsh, and W. T. Frangos. "Permeability of Granite under High Pressure." *Journal of Geophysical Research (1896-1977)* 73 (1968): 2225-2236.

Březina, Jan, a Jan Stebel. „Analysis of Model Error for a Continuum-Fracture Model of Porous Media Flow.“ V *High Performance Computing in Science and Engineering*, 152-160. Springer International Publishing, 2015.

Březina, Jan, Jan Stebel, Pavel Exner, a Jan Hybš. „Flow123d.“ 2011-2016.

Čápová, Lucie. „Specification of the Geothermic Model in the Environs of Several Selected Boreholes.“ Ph.D. dissertation, Charles University in Prague, 2013.

Doonechaly, N. Gholizadeh, R. Abdel Azim, and S. S. Rahman. "Evaluation of Recoverable Energy Potential from Enhanced Geothermal Systems: A Sensitivity Analysis in a Poro-Thermo-Elastic Framework." *Geofluids* 16 (2016): 384-395.

Evans, Lawrence C. *Partial Differential Equations.* American Mathematical Society, 1998.

Ezzedine, Souheil M. "Impact of Geological Characterization Uncertainties on Subsurface Flow Using Stochastic Discrete Fracture Network Models." *Proceedings of the Annual Stanford Workshop on Geothermal Reservoir Engineering.* 2010. 7.

Fisher/Lewis/Embleton. *Statistical Analysis Spherical Data.* Reprint edition. Cambridge: Cambridge University Press, 1993.

—. *Statistical Analysis Spherical Data.* Reprint edition. Cambridge: Cambridge University Press, 1993.

Follin, Sven. "Bedrock Hydrogeology Forsmark – Site Descriptive Modelling, SDM-Site Forsmark." Tech. rep., Svensk K\"arnbr\"anslehantering AB, 2008, 155.

Geuzaine, Christophe, and Jean-François Remacle. "Gmsh: A 3-D Finite Element Mesh Generator with Built-in Pre- and Post-Processing Facilities." *International Journal for Numerical Methods in Engineering* 79 (2009): 1309-1331.

Giles, Michael B. "Multilevel Monte Carlo Methods." *Acta Numerica* 24 (5 2015): 259-328.

INTERA Environmental Consultants, Inc., and T. X. (USA) Houston. "Porosity, Permeability, and Their Relationship in Granite, Basalt, and Tuff." Tech. rep., INTERA Environmental Consultants, Inc., Houston, TX (USA), 1983.

Joyce, Steven, et al. "Groundwater Flow Modelling of Periods with Temperate Climate Conditions – Forsmark." SKB R-09-20, Svensk Kärnbränslehantering AB (n.d.): 315.

Kaviany, Massoud. *Principles of Heat Transfer in Porous Media.* 2nd. Springer, 1999.

Klimczak, Christian, Richard A. Schultz, Rishi Parashar, and Donald M. Reeves. "Cubic Law with Aperture-Length Correlation: Implications for Network Scale Fluid Flow." *Hydrogeology Journal* 18 (6 2010): 851-862.

Ljunggren, Christer, Ove Stephansson, Ove Alm, Hossein Hakami, and Ulf Mattila. "Mechanical Properties of Granitic Rocks from 6IDEÅ, Sweden." Tech. rep., Svensk K\"arnbr\"anslehantering AB, 1985, 80.

Martin, Vincent, Jéro{\textasciicircum}me Jaffré, a Jean E. Roberts. „Modeling Fractures and Barriers as Interfaces for Flow in Porous Media.“ *SIAM Journal on Scientific Computing* 26 (2005): 1667-1691.

Min, Ki-Bok, Lanru Jing, and Ove Stephansson. "Determining the Equivalent Permeability Tensor for Fractured Rock Masses Using a Stochastic REV Approach: Method and Application to the Field Data from Sellafield, UK." *Hydrogeology Journal* 12 (10 2004): 497-510.

Neuman, Shlomo P. "Multiscale Relationships between Fracture Length, Aperture, Density and Permeability." *Geophysical Research Letters* 35 (2008).

Olson, Jon. „Sublinear Scaling of Fracture Aperture versus Length: An Exception or the Rule?“ *J. Geophys. Res* 108 (9 2003).

Rálek, Petr, Josef Novák, Jiří Maryška, and Josef Chudoba. "Numerical Modelling of Deep Geothermal Exchanger and Its Application for the Litoměřice Site, Czech Republic." n.d.: 8.

Rhén, Ingvar, Torbjörn Forsmark, Lee Hartley, Peter Jackson, David Roberts, and Björn Gylling. "Hydrogeological Conceptualisation and Parameterisation – Site Descriptive Modelling. SDM-Site Laxemar." SKB R-08-78, Svensk Kärnbränslehantering AB (n.d.): 745.

Selvadurai, Patrick, Paul Selvadurai, and Morteza Nejati. "A Multi-Phasic Approach for Estimating the Biot Coefficient for Grimsel Granite." *Solid Earth Discussions*, 5 2019: 1-17.

Snow, David T. "Anisotropie Permeability of Fractured Media." *Water Resources Research* 5 (12 1969): 1273-1289.

Šperl, Jan, and Jiřina Trčková. "Permeability and Porosity of Rocks and Their Relationship Based on Laboratory Testing." 5 (2008): 41-47.

Watanabe, Norihiro, Wenqing Wang, Christopher I. McDermott, Takeo Taniguchi, and Olaf Kolditz. "Uncertainty Analysis of Thermo-Hydro-Mechanical Coupled Processes in Heterogeneous Porous Media." *Computational Mechanics* 45 (11 2009): 263.

Zisman, W. A. "Compressibility and Anisotropy of Rocks at and near the Earth's Surface." *Proceedings of the National Academy of Sciences* 19 (7 1933): 666-679.